

University of Nebraska - Lincoln

DigitalCommons@University of Nebraska - Lincoln

---

Kenneth Bloom Publications

Research Papers in Physics and Astronomy

---

11-1-1997


## Determination of the Michel parameters and the $\tau$ neutrino helicity in $\tau$ decay

J.P. Alexander  
*Cornell University*

Kenneth A. Bloom  
*University of Nebraska-Lincoln*, kbloom2@unl.edu

CLEO Collaboration

Follow this and additional works at: <https://digitalcommons.unl.edu/physicsbloom>

 Part of the [Physics Commons](#)

---

Alexander, J.P.; Bloom, Kenneth A.; and Collaboration, CLEO, "Determination of the Michel parameters and the  $\tau$  neutrino helicity in  $\tau$  decay" (1997). *Kenneth Bloom Publications*. 170.  
<https://digitalcommons.unl.edu/physicsbloom/170>

This Article is brought to you for free and open access by the Research Papers in Physics and Astronomy at DigitalCommons@University of Nebraska - Lincoln. It has been accepted for inclusion in Kenneth Bloom Publications by an authorized administrator of DigitalCommons@University of Nebraska - Lincoln.

**Determination of the Michel parameters and the  $\tau$  neutrino helicity in  $\tau$  decay**

J. P. Alexander, C. Bebek, B. E. Berger, K. Berkelman, K. Bloom, D. G. Cassel, H. A. Cho, D. M. Coffman, D. S. Crowcroft, M. Dickson, P. S. Drell, K. M. Ecklund, R. Ehrlich, R. Elia, A. D. Foland, P. Gaidarev, R. S. Galik, B. Gittelman, S. W. Gray, D. L. Hartill, B. K. Heltsley, P. I. Hopman, J. Kandaswamy, P. C. Kim, D. L. Kreinick, T. Lee, Y. Liu, G. S. Ludwig, J. Masui, J. Mevissen, N. B. Mistry, C. R. Ng, E. Nordberg, M. Ogg,\* J. R. Patterson, D. Peterson, D. Riley, A. Soffer, B. Valant-Spaight, and C. Ward  
*Cornell University, Ithaca, New York 14853*

M. Athanas, P. Avery, C. D. Jones, M. Lohner, C. Prescott, J. Yelton, and J. Zheng  
*University of Florida, Gainesville, Florida 32611*

G. Brandenburg, R. A. Briere, Y. S. Gao, D. Y.-J. Kim, R. Wilson, and H. Yamamoto  
*Harvard University, Cambridge, Massachusetts 02138*

T. E. Browder, F. Li, Y. Li, and J. L. Rodriguez  
*University of Hawaii at Manoa, Honolulu, Hawaii 96822*

T. Bergfeld, B. I. Eisenstein, J. Ernst, G. E. Gladding, G. D. Gollin, R. M. Hans, E. Johnson, I. Karliner, M. A. Marsh, M. Palmer, M. Selen, and J. J. Thaler  
*University of Illinois at Champaign-Urbana, Urbana, Illinois 61801*

K. W. Edwards  
*Carleton University, Ottawa, Ontario, Canada K1S 5B6  
and the Institute of Particle Physics, Canada*

A. Bellerive, R. Janicek, D. B. MacFarlane, K. W. McLean, and P. M. Patel  
*McGill University, Montréal, Québec, Canada H3A 2T8  
and the Institute of Particle Physics, Canada*

A. J. Sadoff  
*Ithaca College, Ithaca, New York 14850*

R. Ammar, P. Baringer, A. Bean, D. Besson, D. Coppage, C. Darling, R. Davis, N. Hancock, S. Kotov, I. Kravchenko, and N. Kwak  
*University of Kansas, Lawrence, Kansas 66045*

S. Anderson, Y. Kubota, M. Lattery, S. J. Lee, J. J. O'Neill, S. Patton, R. Poling, T. Riehle, V. Savinov, and A. Smith  
*University of Minnesota, Minneapolis, Minnesota 55455*

M. S. Alam, S. B. Athar, Z. Ling, A. H. Mahmood, H. Severini, S. Timm, and F. Wappler  
*State University of New York at Albany, Albany, New York 12222*

A. Anastassov, S. Blinov,<sup>†</sup> J. E. Duboscq, K. D. Fisher, D. Fujino,<sup>‡</sup> K. K. Gan, T. Hart, K. Honscheid, H. Kagan, R. Kass, J. Lee, M. B. Spencer, M. Sung, A. Undrus,<sup>†</sup> R. Wanke, A. Wolf, and M. M. Zoeller  
*Ohio State University, Columbus, Ohio 43210*

B. Nemati, S. J. Richichi, W. R. Ross, P. Skubic, and M. Wood  
*University of Oklahoma, Norman, Oklahoma 73019*

M. Bishai, J. Fast, E. Gerndt, J. W. Hinson, N. Menon, D. H. Miller, E. I. Shibata, I. P. J. Shipsey, and M. Yurko  
*Purdue University, West Lafayette, Indiana 47907*

L. Gibbons, S. Glenn, S. D. Johnson, Y. Kwon, S. Roberts, and E. H. Thorndike  
*University of Rochester, Rochester, New York 14627*

C. P. Jessop, K. Lingel, H. Marsiske, M. L. Perl, D. Ugolini, R. Wang, and X. Zhou  
*Stanford Linear Accelerator Center, Stanford University, Stanford, California 94309*

T. E. Coan, V. Fadeyev, I. Korolkov, Y. Maravin, I. Narsky, V. Shelkov, J. Staeck, R. Stroynowski,  
I. Volobouev, and J. Ye  
*Southern Methodist University, Dallas, Texas 75275*

M. Artuso, A. Efimov, F. Frasconi, M. Gao, M. Goldberg, D. He, S. Kopp, G. C. Moneti, R. Mountain, S. Schuh,  
T. Skwarnicki, S. Stone, G. Viehhauser, and X. Xing  
*Syracuse University, Syracuse, New York 13244*

J. Bartelt, S. E. Csorna, V. Jain, and S. Marka  
*Vanderbilt University, Nashville, Tennessee 37235*

R. Godang, K. Kinoshita, I. C. Lai, P. Pomianowski, and S. Schrenk  
*Virginia Polytechnic Institute and State University, Blacksburg, Virginia 24061*

G. Bonvicini, D. Cinabro, R. Greene, L. P. Perera, and G. J. Zhou  
*Wayne State University, Detroit, Michigan 48202*

B. Barish, M. Chadha, S. Chan, G. Eigen, J. S. Miller, C. O'Grady, M. Schmidtler, J. Urheim,  
A. J. Weinstein, and F. Würthwein  
*California Institute of Technology, Pasadena, California 91125*

D. M. Asner, D. W. Bliss, W. S. Brower, G. Masek, H. P. Paar, S. Prell, and V. Sharma  
*University of California, San Diego, La Jolla, California 92093*

J. Gronberg, T. S. Hill, R. Kutschke, D. J. Lange, S. Menary, R. J. Morrison, H. N. Nelson, T. K. Nelson, C. Qiao,  
J. D. Richman, D. Roberts, A. Ryd, and M. S. Witherell  
*University of California, Santa Barbara, California 93106*

R. Balest, B. H. Behrens, K. Cho, W. T. Ford, H. Park, P. Rankin, J. Roy, and J. G. Smith  
*University of Colorado, Boulder, Colorado 80309-0390*

(CLEO Collaboration)  
(Received 15 May 1997)

Using the CLEO II detector at the Cornell Electron Storage Ring operated at  $\sqrt{s}=10.6$  GeV, we have determined the Michel parameters  $\rho$ ,  $\xi$ , and  $\delta$  in  $\tau^\pm \rightarrow l^\pm \nu \bar{\nu}$  decay as well as the  $\tau$  neutrino helicity parameter  $h_{\nu_\tau}$  in  $\tau^\pm \rightarrow \pi^\mp \pi^0 \nu$  decay. From a data sample of  $3.02 \times 10^6$  produced  $\tau$  pairs we analyzed events of the topologies  $e^+ e^- \rightarrow \tau^+ \tau^- \rightarrow (l^\pm \nu \bar{\nu})(\pi^\mp \pi^0 \nu)$  and  $e^+ e^- \rightarrow \tau^+ \tau^- \rightarrow (\pi^\pm \pi^0 \bar{\nu})(\pi^\mp \pi^0 \nu)$ . We obtain  $\rho = 0.747 \pm 0.010 \pm 0.006$ ,  $\xi = 1.007 \pm 0.040 \pm 0.015$ ,  $\xi\delta = 0.745 \pm 0.026 \pm 0.009$ , and  $h_{\nu_\tau} = -0.995 \pm 0.010 \pm 0.003$ , where we have used the previously determined sign of  $h_{\nu_\tau}$  [ARGUS Collaboration, H. Albrecht *et al.*, *Z. Phys. C* **58**, 61 (1993); *Phys. Lett. B* **349**, 576 (1995)]. We also present the Michel parameters as determined from the electron and muon samples separately. All results are in agreement with the standard model  $V-A$  interaction. [S0556-2821(97)06819-7]

PACS number(s): 13.35.Dx, 14.60.Fg

## I. INTRODUCTION

The most general, local, derivative-free, and lepton-number-conserving four-fermion point interaction [1–3] for leptonic  $\tau$  decays yields in the helicity projection form [4] the matrix element

$$\mathcal{M} = 4 \frac{G_I}{\sqrt{2}} \sum_{\substack{\gamma=S,V,T \\ \epsilon,\mu=R,L}} g_{\epsilon\mu}^\gamma [\bar{u}_\epsilon(l^-) \Gamma_\gamma \nu_j(\bar{\nu}_l)] [\bar{u}_i(\nu_\tau) \Gamma^\gamma u_\mu(\tau^-)], \quad (1)$$

where  $G_I$  parametrizes the total strength of the interaction and  $l$  refers to  $e$  or  $\mu$ . The matrices  $\Gamma_\gamma$  define the properties of the two currents under a Lorentz transformation with  $\gamma=S, V, T$  for scalar, vector, and tensor interactions. The indices  $\epsilon$  and  $\mu$  label the right or left handedness ( $R, L$ ) of the charged leptons. For a given  $\epsilon, \mu$ , and  $\gamma$ , the handedness of the neutrinos labeled by  $j$  and  $i$  are fixed. Only ten of the twelve complex coupling constants  $g_{\epsilon\mu}^\gamma$  are linearly independent. In the standard model  $V-A$  interaction, the only non-zero coupling constant is  $g_{LL}^V = 1$ .

\*Permanent address: University of Texas, Austin, TX 78712.

†Permanent address: BINP, RU-630090 Novosibirsk, Russia.

‡Permanent address: Lawrence Livermore National Laboratory, Livermore, CA 94551.

The interaction described by Eq. (1) is fully determined by 19 real parameters. Without measuring the neutrinos and the spin of the outgoing charged lepton, only the four Michel parameters [1–3]  $\rho$ ,  $\eta$ ,  $\xi$ , and  $\delta$  are experimentally accessible. They are bilinear combinations of the coupling constants  $g_{\epsilon\mu}^\gamma$  and appear in the predicted energy spectrum of the charged lepton  $l^\mp$  emitted in the decay  $\tau^\mp \rightarrow l^\mp \nu \bar{\nu}$ . In the  $\tau$  rest frame, neglecting radiative corrections and terms proportional to  $m_l^2/m_\tau^2$ , this spectrum is given by

$$\begin{aligned} \frac{d\Gamma(\tau^\mp \rightarrow l^\mp \nu \bar{\nu})}{d\Omega dx} &= \frac{G_F^2 m_\tau^5}{192\pi^4} x^2 \left( 3(1-x) + \frac{2}{3}\rho(4x-3) \right. \\ &\quad \left. + 6\eta \frac{m_l}{m_\tau} \frac{1-x}{x} \mp \xi \mathcal{P}_\tau \cos\theta \left[ (1-x) \right. \right. \\ &\quad \left. \left. + \frac{2}{3}\delta(4x-3) \right] \right), \end{aligned} \quad (2)$$

where  $x=2E_l/m_\tau$  is the scaled charged lepton energy,  $\mathcal{P}_\tau$  the  $\tau$  polarization, and  $\theta$  the angle between  $\tau$  spin and lepton momentum. The standard model  $V-A$  charged weak current is characterized by  $\rho=3/4$ ,  $\eta=0$ ,  $\xi=1$ , and  $\delta=3/4$ .

A measurement of the Michel parameters allows one to limit the coupling constants  $g_{\epsilon\mu}^\gamma$ . For example,  $\xi$  and  $\delta$  determine the probability  $P_R^\tau$  for a right-handed  $\tau$  lepton to participate in leptonic  $\tau$  decays:

$$\begin{aligned} P_R^\tau &= \frac{1}{4} |g_{RR}^S|^2 + \frac{1}{4} |g_{LR}^S|^2 + |g_{RR}^V|^2 + |g_{LR}^V|^2 + 3|g_{LR}^T|^2 \\ &= \frac{1}{2} [1 + \frac{1}{9}(3\xi - 16\xi\delta)]. \end{aligned} \quad (3)$$

In semihadronic  $\tau$  decays the strong interaction imposes constraints on the general form of the matrix element. Depending on the quantum numbers of the intermediate hadronic state, some of the interactions taken into account by Eq. (1) are forbidden. For the decay  $\tau^\mp \rightarrow \pi^\mp \pi^0 \nu$ , with a vector meson as the intermediate hadronic state, only vector and axial vector interactions are possible. Denoting the vector coupling by  $g_V$  and the axial vector coupling by  $g_A$ , the general matrix element for the decay  $\tau^\mp \rightarrow \pi^\mp \pi^0 \nu$  can be parametrized by  $h_{\nu_\tau} = 2g_V g_A / (g_V^2 + g_A^2)$ . The parameter  $h_{\nu_\tau}$  is proportional to the  $\tau$  neutrino helicity. In the standard model, with purely left-handed neutrinos, one expects  $h_{\nu_\tau} = -1$ . Omitting the total strength of the interaction and other constant factors, the general matrix element is [5]

$$\begin{aligned} |\mathcal{M}(\tau^\mp \rightarrow \pi^\mp \pi^0 \nu)|^2 &\propto H \pm h_{\nu_\tau} (sH') \\ &= 2(kQ)(qQ) - (kq)(QQ) \pm m_\tau h_{\nu_\tau} s_\mu \\ &\quad \times [2Q^\mu(kQ) - k^\mu(QQ)], \end{aligned} \quad (4)$$

where the four-vectors  $k$ ,  $q$ ,  $s$ , and  $Q$  denote the  $\tau$  neutrino momentum, the  $\tau$  momentum, the  $\tau$  spin vector, and  $p_{\pi^\mp} - p_{\pi^0}$ , respectively. Using the shorthand notations  $H$  and  $H'$ , the polarimeter vector of the decay is  $h_\mu = H'_\mu / H$  [5,6]. In the  $\tau$  rest frame only the three-vector  $\vec{h}$  of the polarimeter vector is relevant, where  $\vec{h}$  is aligned to the expected spin direction of the decay products.

Despite the progress made in recent years [7–18], the determination of the space-time structure in leptonic and semihadronic  $\tau$  decays is still an order of magnitude less precise than in  $\mu$  decay. This indicates a need for high-precision measurements of the Michel parameters in leptonic  $\tau$  decays as well as of the  $\tau$  neutrino helicity in semihadronic  $\tau$  decays. In this paper, we present measurements of  $\rho$ ,  $\xi$ ,  $\delta$ , and the  $\tau$  neutrino helicity parameter  $h_{\nu_\tau}$  from an analysis of  $e^+e^- \rightarrow \tau^+\tau^- \rightarrow (l^\pm \nu \bar{\nu})(\pi^\mp \pi^0 \nu)$  and  $(\pi^\pm \pi^0 \bar{\nu})(\pi^\mp \pi^0 \nu)$  events.

The  $(l^\pm \nu \bar{\nu})(\pi^\mp \pi^0 \nu)$  sample used here is correlated with that of Ref. [17]. There, the Michel parameters  $\rho$  and  $\eta$  were determined with emphasis on a precise measurement of  $\eta$ , in which the sensitivity comes mainly from the low-momentum part of the muon spectrum. Here, the emphasis lies on the determination of the spin-dependent Michel parameters  $\xi$  and  $\delta$ .

## II. METHOD OF THE MEASUREMENT

Equation (2) shows that the measurement of  $\xi$  and  $\delta$  requires the knowledge of the  $\tau$  spin orientation. In  $e^+e^-$  annihilation at  $\sqrt{s} \approx 10$  GeV the average  $\tau$  polarization is zero and no information on  $\xi$  and  $\delta$  can be obtained from single  $\tau$  decays. However, spin-spin correlations exist between the two  $\tau$  leptons in  $e^+e^- \rightarrow \tau^+\tau^-$ , leading to correlations between kinematical properties of the decay products. These correlations have been used before [8,10,12] for the determination of  $\xi$ ,  $\delta$ , and  $h_{\nu_\tau}$ , where leptonic as well as semihadronic decays served as spin analyzers. Here we use the semihadronic  $\tau$  decay  $\tau^\mp \rightarrow \pi^\mp \pi^0 \nu$  as spin analyzer. Its advantages are a large branching fraction, a very well understood hadronic current, and an experimentally clean signal.

In the Born approximation, the matrix element for the differential cross section of  $e^+e^- \rightarrow \tau^+\tau^- \rightarrow (l^\pm \nu \bar{\nu})(\pi^\mp \pi^0 \nu)$  has, after integration over the unobserved neutrino degrees of freedom and summation over unobserved spins, the structure (see, for example, Ref. [19])

$$|\mathcal{M}|^2 = HP[E_1 + \rho E_2 + \eta E_3] + h_{\nu_\tau} H'_\alpha C^{\alpha\beta} [\xi E'_{1\beta} + \xi \delta E'_{2\beta}]. \quad (5)$$

The first term is the spin-averaged part of the differential cross section. The second term contains the spin correlation. As defined by Eq. (4),  $H$  is the spin-averaged part of the matrix element for the semihadronic decay  $\tau^\mp \rightarrow \pi^\mp \pi^0 \nu$ , whereas  $H'$  is the spin-dependent part. The symbols  $E_i$  and  $E'_i$  are the Lorentz invariant formulations of the corresponding terms in Eq. (2). The spin-averaged  $\tau$  pair production is denoted by  $P$  and the production spin correlation matrix by  $C^{\alpha\beta}$ .

The spin analyzer  $\tau^\mp \rightarrow \pi^\mp \pi^0 \nu$  can resolve the ratio of longitudinal to transverse polarization of the intermediate  $\rho$  meson, but, because of the absence of interference terms, cannot separate its transverse polarization into the left- and right-handed part. Thus our  $(l^\pm \nu \bar{\nu})(\pi^\mp \pi^0 \nu)$  events are sensitive to  $\rho$ ,  $\eta$ ,  $h_{\nu_\tau} \xi$ , and  $h_{\nu_\tau} \xi \delta$  [see Eq. (5)], whereas our  $(\pi^\pm \pi^0 \bar{\nu})(\pi^\mp \pi^0 \nu)$  events allow a determination of the

product  $h_{\nu_\tau}^2$ . The signs of  $\xi$  and  $h_{\nu_\tau}$  are well known from other experiments [7,8] and no attempt is made to remeasure them in this analysis.

Not all of the kinematical quantities needed to evaluate Eq. (5) for each detected event are well determined. For example, the azimuthal angle of the unmeasured  $\tau$  momentum around the two-pion momentum can take on a range of values, restricted by kinematical constraints. Initial-state radiation, radiative corrections to the decays  $\tau^\pm \rightarrow l^\pm \bar{\nu} \nu$  and  $\tau^\pm \rightarrow \pi^\mp \pi^0 \nu$ , external bremsstrahlung, and uncertainties of the measured momenta will also modify the evaluation of Eq. (5).

We determine the Michel parameters from a single event likelihood fit to the selected data samples. The indeterminacies described above are taken into account in the likelihood function by forming a weighted sum over all possible kinematical configurations. The weights are derived by assuming that radiative effects and the detector resolution factorize from the Born level matrix element and do not depend on the fit parameters. Formally, the per event likelihood function is taken to be

$$L(\Theta|\vec{a}) \equiv P(\vec{a}|\Theta) = \frac{\int |\mathcal{M}(\vec{\alpha}, \vec{\beta}|\Theta)|^2 \eta(\vec{\alpha}) w(\vec{a}, \vec{\beta}|\vec{\alpha}) d\vec{\beta} d\vec{\alpha}}{\int |\mathcal{M}(\vec{\alpha}, \vec{\beta}|\Theta)|^2 \eta(\vec{\alpha}) w(\vec{a}, \vec{\beta}|\vec{\alpha}) d\vec{\beta} d\vec{\alpha} d\vec{a}}, \quad (6)$$

where  $|\mathcal{M}|^2$  is given by Eq. (5). The vector  $\Theta$  represents the set of parameters  $(\rho, \eta, h_{\nu_\tau}, \xi, h_{\nu_\tau}, \xi, \delta)$  that are determined in the fit. As discussed below, we also include the  $\Theta$  dependence of all significant sources of background in the event likelihood. The vector  $\vec{a}$  contains all measured quantities, i.e., the momenta of the charged lepton and the two pions. The vector  $\vec{\beta}$  contains all unmeasured quantities, such as those associated with the neutrinos, the photons of the initial-state bremsstrahlung that mostly escape undetected down the beam pipe, radiated photons in the decay, and photons from external bremsstrahlung. The vector  $\vec{\alpha}$  represents the value of the measured quantities before resolution and radiative effects. The weight  $w(\vec{a}, \vec{\beta}|\vec{\alpha})$  contains all of the resolution and radiative effects, and the integrals over  $\vec{\alpha}$  perform convolutions with the detector resolution. The acceptance function of the detector is denoted by  $\eta$  and depends only on  $\vec{\alpha}$ . The denominator in Eq. (6) ensures that the likelihood integrated over  $\vec{a}$  is normalized to unity for all values of  $\Theta$ .

The integration over the unmeasured quantities is done analytically as far as possible. The remaining integration is most conveniently computed numerically using Monte Carlo methods. In the Monte Carlo algorithm used here, many trials are executed for each observed event to generate the unmeasured quantities  $\vec{\beta}$  (radiated photons) and the ‘‘before radiation and detector resolution’’ values  $\vec{\alpha}$  of the measured quantities. Not all trials are successful in generating  $\vec{\beta}$  and  $\vec{\alpha}$  consistent with the kinematics of  $\tau$  pair events. We have chosen the number of trials to be 450 such that the number of successful trials for most signal events is large enough to achieve adequate precision for this integration. (In addition, the fraction of trials that are successful  $f_{\text{hit}}$  is a measure of the goodness of the hypothesis that the event is a  $\tau$  pair.) The

Monte Carlo integration over the measurable quantities  $\vec{a}$  in the denominator of Eq. (6) is done with a full detector simulation. This technique was used in Ref. [8]. Here we have applied only minor changes, such as taking the radiative corrections in the semihadronic decay into account. A full description can be found in Ref. [20].

The effectiveness of this technique has been demonstrated by generating events with the KORALB/TAUOLA [5,21] Monte Carlo program and applying the fit method to these events. The results are compatible with the input within the statistical errors of the test, which are of order 0.01%. These tests have been performed for standard model input values as well as for non-standard-model values. Thus, at the level of accuracy needed here, we have demonstrated that the method is unbiased and the factorization assumption mentioned above is justified.

### III. DATA SELECTION

The measurements presented here were performed with the CLEO II detector [22] at the Cornell Electron Storage Ring. The data sample used here was collected at center of mass energies around  $\sqrt{s} = 10$  GeV. The integrated luminosity is  $\approx 3.5 \text{ fb}^{-1}$ , with about  $3.02 \times 10^6$   $\tau$  pairs produced.

Events with exactly two oppositely charged tracks are selected. Each track must have a momentum greater than 500 MeV/ $c$  and its distance of closest approach to the interaction point in the plane transverse to the beam must be less than 10 mm. The polar angle of each track relative to the beam must satisfy the condition  $|\cos \theta| < 0.71$ . The two tracks are required to be separated by an opening angle of more than  $90^\circ$ .

To suppress non- $\tau$  background we require that not more than one of the two tracks has a momentum greater than 85% of the beam energy. The total energy (due to photons, showers associated with charged tracks, and all other sources) measured in the electromagnetic calorimeter has to be greater than 20% and less than 85% of  $\sqrt{s}$ . Additionally, the momenta  $\vec{p}_i$  of the two tracks have to satisfy the condition  $|\vec{p}_1 + \vec{p}_2| / (|\vec{p}_1| + |\vec{p}_2|) > 0.05$  to suppress cosmic rays.

We reconstruct  $\pi^0 \rightarrow \gamma\gamma$  decays using calorimeter showers that are not matched to a charged track, with an energy greater than 50 MeV and a polar angle of  $|\cos \theta| < 0.71$ . To suppress background from  $\tau$  decays with more  $\pi^0$  mesons than the mode under study, we reject events containing additional showers that are not associated with a reconstructed  $\pi^0$  meson, that lie more than 30 cm from the closest charged track projection into the calorimeter, and that have energies of more than 75 MeV for polar angles of  $|\cos \theta| < 0.71$  and 100 MeV for  $|\cos \theta| > 0.71$ .

In the lepton-versus- $\rho$  sample exactly one  $\pi^0$  is required with  $-4 < (m_{\gamma\gamma} - m_{\pi^0}) / \sigma_{m_{\gamma\gamma}} < 3$ , where the mass resolution  $\sigma_{m_{\gamma\gamma}}$  is typically between 5 MeV/ $c^2$  and 10 MeV/ $c^2$  depending on the  $\pi^0$  energy. The momentum of the reconstructed  $\pi^0$  has to be greater than 300 MeV/ $c$ .

The track further away in angle from the reconstructed  $\pi^0$  is required to be either an electron or a muon. Tracks are identified as electrons when their momentum and  $dE/dx$  information from the tracking system, as well as the energy measurement in the electromagnetic calorimeter, are consis-

TABLE I. Background contribution from other  $\tau$  decays.

| Electrons, 33 531 Accepted events                |                          | Muons, 21 680 Accepted events                      |                          | $\rho$ mesons, 11 177 Accepted events                |                          |
|--|--------------------------|--|--------------------------|--|--------------------------|
| Event topology                                   | Estimated background (%) | Event topology                                     | Estimated background (%) | Event topology                                       | Estimated background (%) |
| $(e^\pm \nu \bar{\nu})(\pi^\mp \pi^0 \pi^0 \nu)$ | $1.78 \pm 0.20$          | $(\mu^\pm \nu \bar{\nu})(\pi^\mp \pi^0 \pi^0 \nu)$ | $1.73 \pm 0.20$          | $(\pi^\pm \pi^0 \bar{\nu})(\pi^\mp \pi^0 \pi^0 \nu)$ | $3.95 \pm 0.45$          |
| $(e^\pm \nu \bar{\nu})(K^\mp \pi^0 \nu)$         | $1.94 \pm 0.20$          | $(\mu^\pm \nu \bar{\nu})(K^\mp \pi^0 \nu)$         | $2.00 \pm 0.20$          | $(\pi^\pm \pi^0 \bar{\nu})(K^\mp \pi^0 \nu)$         | $4.31 \pm 0.50$          |
| $(\pi^\pm \bar{\nu})(\pi^\mp \pi^0 \nu)$         | $0.14 \pm 0.03$          | $(\pi^\pm \bar{\nu})(\pi^\mp \pi^0 \nu)$           | $1.29 \pm 0.18$          |  |                          |
| $(e^\pm \nu \bar{\nu})(\pi^\mp \nu)$             | $0.13 \pm 0.02$          | $(\mu^\pm \nu \bar{\nu})(\pi^\mp \nu)$             | $0.14 \pm 0.03$          |  |                          |
| remaining sources                                | $0.96 \pm 0.10$          | remaining sources                                  | $0.90 \pm 0.10$          | remaining sources                                    | $2.04 \pm 0.20$          |
| $\Sigma$   | $4.95 \pm 0.30$          | $\Sigma$   | $6.06 \pm 0.35$          | $\Sigma$   | $10.30 \pm 0.70$         |

tent with the electron hypothesis. Tracks with momenta greater than 1.5 GeV/ $c$  are identified as muons if they match to hits in the muon counters beyond at least three absorption lengths of material.

The invariant mass of the reconstructed  $\pi^0$  and the charged pion candidate has to satisfy  $m_{\pi^\mp \pi^0} > 0.5$  GeV/ $c^2$ . The missing mass  $m_{\text{miss}}$  of the event has to satisfy the condition  $m_{\text{miss}} > 0.1\sqrt{s}$ . Additionally, we require the Monte Carlo success rate  $f_{\text{hit}}$  (see Sec. II) to be at least 6.6%. After these three cuts the remaining background from Bhabha events, two-photon interactions, and  $q\bar{q}$  events is negligible, as has been verified by a careful comparison of relevant kinematical distributions between data and  $\tau$  pair Monte Carlo events (KORALB/TAUOLA [5,21]). For  $q\bar{q}$  background this has also been confirmed by an analysis of  $q\bar{q}$  Monte Carlo events.

In the  $\rho$ -versus- $\rho$  sample exactly two  $\pi^0$  mesons are required with  $-4 < (m_{\gamma\gamma} - m_{\pi^0})/\sigma_{m_{\gamma\gamma}} < 3$ . A momentum cut of greater than 300 MeV/ $c$  is applied on the reconstructed  $\pi^0$  mesons. The  $\pi^0$  mesons are associated with the charged tracks by their nearness in angle. The invariant masses  $m_{\pi^\mp \pi^0}$  of the  $\rho$  meson candidates have to be greater than 0.5 GeV/ $c^2$ . These cuts are identical to those used in the  $l$ -vs- $\rho$  selection and suppress backgrounds from  $\tau$  pair events with different decay modes. In addition, the missing transverse momentum of the event,  $p_T$ , and  $E_{\text{tot}}$ , the total energy of the observed particles, have to satisfy  $p_T/(\sqrt{s} - E_{\text{tot}}) > 0.1$ ,  $p_T/(\sqrt{s}/2) > 0.075$ , and  $E_{\text{tot}}/\sqrt{s} > 0.3$ . We again require  $f_{\text{hit}} > 6.6\%$ . We verified with Monte Carlo studies, as described in the preceding paragraph, that after these cuts the contribution from non- $\tau$  background is negligible.

This selection results in a sample of 66 388 accepted events, comprising 33 531 candidates in the topology  $(e^\mp \nu \bar{\nu})(\pi^\pm \pi^0 \bar{\nu})$ , 21 680 candidates in  $(\mu^\mp \nu \bar{\nu})(\pi^\pm \pi^0 \bar{\nu})$ , and 11 177 candidates in  $(\pi^\mp \pi^0 \nu)(\pi^\pm \pi^0 \bar{\nu})$ . These numbers of events are in good agreement with expectations based on world average branching ratios [23].

In all three samples,  $e$  vs  $\rho$ ,  $\mu$  vs  $\rho$ , and  $\rho$  vs  $\rho$ , the background from non- $\tau$  events is insignificant. The background from  $\tau$  events is estimated by using the KORALB/TAUOLA Monte Carlo program [5,21]. The results are listed in Table I, where the errors reflect statistical, experimental, and theoretical uncertainties. The total contribution from  $\tau$  background is about 5% for  $(e^\mp \nu \bar{\nu})(\pi^\pm \pi^0 \bar{\nu})$ , around 6% for  $(\mu^\mp \nu \bar{\nu})(\pi^\pm \pi^0 \bar{\nu})$ , and approximately 10% for

$(\pi^\mp \pi^0 \nu)(\pi^\pm \pi^0 \bar{\nu})$  events. The ‘‘remaining sources’’ (Table I) are from a variety of modes.

#### IV. DATA ANALYSIS

The spin correlation used in this analysis can be most easily illustrated with the spin sensitive variable  $\omega$  [24] of the decay  $\tau^\mp \rightarrow \pi^\mp \pi^0 \nu$ . In the  $\tau$  rest frame, assuming the standard model  $V-A$  interaction ( $h_{\nu_\tau} = -1$ ), the matrix element given by Eq. (4) can be written as

$$|\mathcal{M}(\tau^\mp \rightarrow \pi^\mp \pi^0 \nu)|^2 \propto H(1 \pm s_z h_z), \quad (7)$$

where the  $z$  axis has been chosen as spin quantization axis. The symbols  $s_z$  and  $h_z$  denote the  $z$  components of the  $\tau$  spin vector and the polarimeter vector introduced in Sec. I [ $s_z$  is just the longitudinal  $\tau$  polarization and is equivalent to  $\mathcal{P}_\tau$  in Eq. (2)].

In the case where the  $\tau$  flight direction is chosen as the  $z$  axis, i.e., the spin quantization axis, left-handed  $\tau$  leptons correspond to  $s_z < 0$  and right-handed  $\tau$  leptons to  $s_z > 0$ . With this, Eq. (7) shows that left-handed  $\tau^-$  leptons (right-handed  $\tau^+$  leptons) have preferentially negative- $h_z$  values, whereas right-handed  $\tau^-$  leptons (left-handed  $\tau^+$  leptons) have preferentially positive- $h_z$  values. Averaging  $h_z$  over the kinematically allowed  $\tau$  rest frames yields the variable  $\omega$  (i.e., integrating over the azimuthal angle of the  $\tau$  momentum around the two-pion momentum).

Figure 1 shows the dependence of the measured electron momentum spectrum on  $\omega$ . One clearly sees that for negative- $\omega$  values, high-momentum leptons are preferred by the data, whereas for positive- $\omega$  values, low-momentum leptons are preferred. This correlation indicates  $h_{\nu_\tau} \xi \approx -1$ , as expected by the standard model. For  $h_{\nu_\tau} \xi = 0$ , which is equivalent to zero spin correlation, the lepton momentum spectrum is independent of  $\omega$ , as can be seen in Fig. 1. The plots corresponding to Fig. 1 for the  $\mu$ -vs- $\rho$  sample are very similar and are not shown here. Figure 2 shows for the  $\rho$ -vs- $\rho$  sample the  $\omega$  spectrum of one side of the event for different values of  $\omega$  from the other side (two entries per event). Again the data favor  $h_{\nu_\tau}^2 \approx 1$ , in agreement with the standard model.

To take the background from other  $\tau$  events into account, the fit function of Eq. (6) is extended to include background:

$$L_i = [1 - (\alpha_1 + \dots + \alpha_n)] S_i + \alpha_1 B_{1,i} + \dots + \alpha_n B_{n,i}, \quad (8)$$

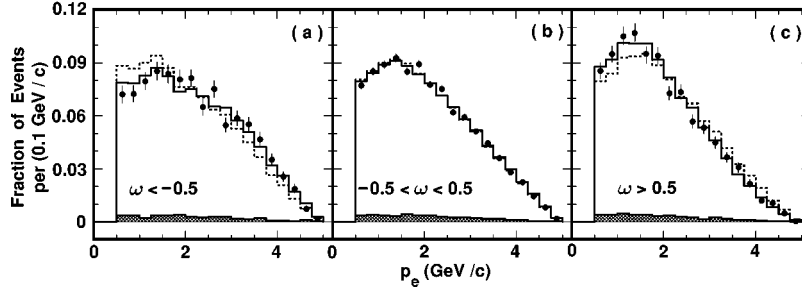


FIG. 1. Electron momentum spectrum in different regions of  $\omega$ . The variable  $\omega$  is sensitive to the spin of the  $\tau$  lepton in the decay  $\tau^\mp \rightarrow \pi^\mp \pi^0 \nu$  ( $\omega < 0 \Rightarrow \tau^-$  left handed,  $\omega > 0 \Rightarrow \tau^-$  right handed). The data (points with errors) as well as the Monte Carlo expectation for  $h_{\nu_\tau} \xi = -1$  (solid histograms) show clearly the spin correlation, whereas for  $h_{\nu_\tau} \xi = 0$  (dashed histograms) the two sides of the event are uncorrelated. The hatched histograms show the Monte Carlo predicted background (assuming  $h_{\nu_\tau} \xi = -1$ ).

where  $\alpha_k$  is the background fraction of the  $k$ th background. The function  $S_i$  is the likelihood of the  $i$ th signal event, given by Eq. (6). The functions  $B_{k,i}$  are the corresponding likelihoods of the backgrounds. For the dominant sources of background, listed in Table I, the functions  $B_{k,i}$  include their full dependence on the fit parameters  $\Theta$  to avoid bias. The values used in the fits for the background fractions  $\alpha_k$  are taken from Table I. The amount of background not included in the fit is  $\approx 1\%$  in the  $l$ -vs- $\rho$  sample and around 2% in the  $\rho$ -vs- $\rho$  sample. The effect of this disregarded background (“remaining sources” in Table I) is discussed in the systematic error section.

The hadronic current of the spin analyzer  $\tau^\mp \rightarrow \pi^\mp \pi^0 \nu$  is very well known. However, the  $q^2$  dependence of the intermediate resonance structure might be a possible source for uncertainties, especially the contribution of the  $\rho'$  meson. The  $\rho'$  contribution is parametrized by  $\beta$  [25], and with  $e^+e^-$  data [26]  $\beta$  is determined [25] to be  $\beta = -0.145$ . In a recent CLEO measurement [27], where  $\tau$  events were used, a value of  $\beta = -0.091 \pm 0.009$  was measured. For consistency, we use the latter value together with the mass and width obtained in Ref. [27] for the  $\rho$  and  $\rho'$  mesons.

The only fit parameter in the  $\rho$ -vs- $\rho$  analysis is  $h_{\nu_\tau}^2$ . We obtain

$$h_{\nu_\tau}^2 = 0.989 \pm 0.019.$$

In the  $e$ -vs- $\rho$  analysis we have three fit parameters  $\rho$ ,  $h_{\nu_\tau} \xi$ , and  $h_{\nu_\tau} \xi \delta$ . We measure the values

$$\rho_e = 0.747 \pm 0.012, \quad h_{\nu_\tau} \xi_e = 0.973 \pm 0.047,$$

$$h_{\nu_\tau} \xi_e \delta_e = 0.716 \pm 0.031.$$

As mentioned in the Introduction, the  $l$ -vs- $\rho$  sample used here is correlated with the one used in Ref. [17]. Because of the special treatment of the low-energy muons there, the precision on the Michel parameter  $\eta$  reached in Ref. [17] is better than the one we might obtain here. Therefore, we do not fit for  $\eta$ . Instead we fixed  $\eta$  to the value determined in Ref. [17] of  $\eta_\mu = 0.010 \pm 0.261$  and  $\eta_\mu = -0.015 \pm 0.091$ , where the first result is obtained in the muon sample alone and the second one is the combined result of the muon and electron sample under the assumption  $\rho_e = \rho_\mu$ . With the first result we obtain, in the  $\mu$ -vs- $\rho$  analysis,

$$\rho_\mu = 0.750 \pm 0.017, \quad h_{\nu_\tau} \xi_\mu = 1.048 \pm 0.068,$$

$$h_{\nu_\tau} \xi_\mu \delta_\mu = 0.781 \pm 0.040.$$

Using the second result we measure, with the  $\mu$ -vs- $\rho$  sample,

$$\rho_\mu = 0.746 \pm 0.017, \quad h_{\nu_\tau} \xi_\mu = 1.043 \pm 0.067,$$

$$h_{\nu_\tau} \xi_\mu \delta_\mu = 0.777 \pm 0.040.$$

All errors shown above are statistical only. Fixing  $\eta$  to the standard model value of  $\eta = 0$  results in shifts of  $\rho_{\eta = -0.015} - \rho_{\eta = 0} = -0.0029$ ,  $(h_{\nu_\tau} \xi)_{\eta = -0.015}$

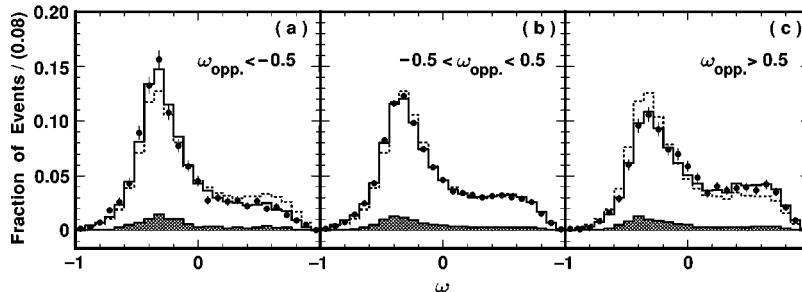


FIG. 2.  $\omega$  spectrum for the  $\rho$ -vs- $\rho$  sample of one side of the event for different values of  $\omega$  from the other side (two entries per event). The data are represented by the dots with error bars. The solid histograms show the Monte Carlo expectation for  $h_{\nu_\tau}^2 = 1$ . The Monte Carlo expectation for  $h_{\nu_\tau}^2 = 0$  is given by the dashed histograms. Background is indicated by the hatched histograms (assuming  $h_{\nu_\tau}^2 = 1$ ).

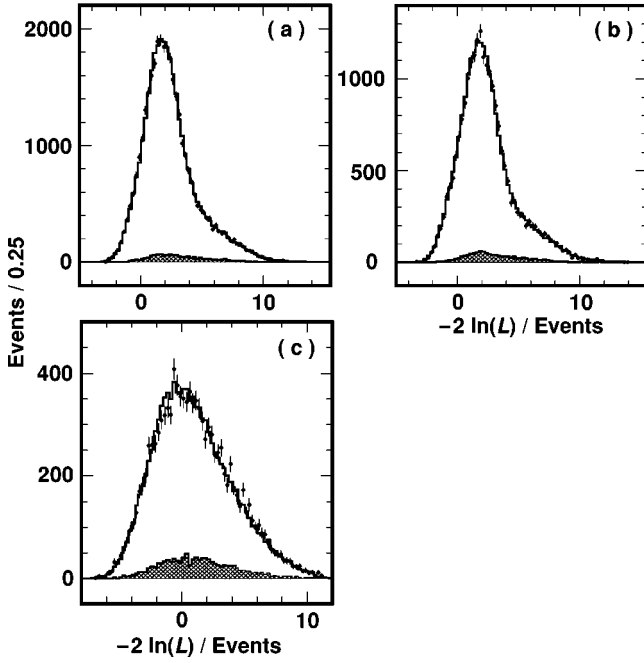


FIG. 3. Contributions of single events to  $-2 \ln L$  for (a)  $(e^+ \nu \bar{\nu})(\pi^+ \pi^0 \bar{\nu})$ , (b)  $(\mu^+ \nu \bar{\nu})(\pi^+ \pi^0 \bar{\nu})$ , and (c)  $(\pi^+ \pi^0 \nu) \times (\pi^+ \pi^0 \bar{\nu})$  events. Data (dots with error bars) and Monte Carlo estimate (solid histograms) are in good agreement. Background is represented by the hatched histograms.

$$-(h_{\nu\tau}\xi)_{\eta=0} = -0.0024, \text{ and } (h_{\nu\tau}\xi\delta)_{\eta=-0.015} - (h_{\nu\tau}\xi\delta)_{\eta=0} = -0.0018.$$

The confidence levels of the fits are 73% in the  $e$ -vs- $\rho$  analysis, 21% in the  $\mu$ -vs- $\rho$  analysis, and 9% in the  $\rho$ -vs- $\rho$  analysis. Figure 3 shows the corresponding log likelihood per event distributions. One sees that the data are in good agreement with the best-fit model.

Systematic errors arise from statistical errors of the Monte Carlo estimate of the normalization integral and from uncertainties in the momentum dependence of the lepton identification efficiency, the acceptance function of the  $\pi^+ \pi^0$  spin analyzer, the background estimates, the model for the hadronic current, the detector resolution, the radiative corrections, and the trigger efficiencies. The different contributions to the systematic error are summarized in Table II.

The lepton identification efficiency has been measured, as a function of momentum and polar angle, with independent lepton data samples. The systematic error given in Table II arises from the statistical error of this measurement. The acceptance function of the  $\pi^+ \pi^0$  spin analyzer has been varied via its dependence on the momenta of the two pions and the angle between the two pions. The variations considered have been determined by comparison of the Monte Carlo estimate and data. The systematic error due to the considered background has been evaluated by varying the fractions of the different backgrounds in the fit function over a range given by statistical, experimental, and theoretical uncertainties. The effect of the disregarded background has been studied using the Monte Carlo estimate. The  $\rho'$  contribution is measured in Ref. [27] with an error of  $\Delta\beta = \pm 0.009$ . Since  $\beta$  has model dependences, and to be conservative, we varied  $\beta$  in the range of  $\pm 0.020$ . The systematic error due to  $\eta$  has been evaluated by varying  $\eta$  within its determined range [17]. The

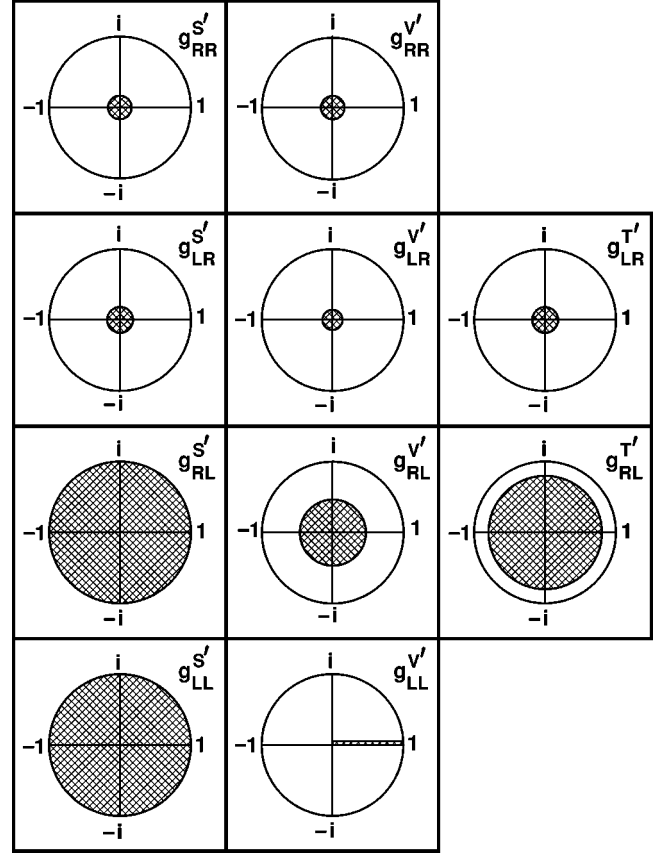


FIG. 4. 90% confidence limits on the reduced coupling constants  $g_{\epsilon\mu}^{\gamma'} = g_{\epsilon\mu}^{\gamma} / \max(g_{\epsilon\mu}^{\gamma})$ .

uncertainty in the detector resolution has been estimated by scaling the error matrix of the resolution by a factor of 4. The systematic error due to radiation has been obtained by varying the amount of radiation in the fit function by  $\pm 10\%$ . The uncertainty in the trigger efficiency arises from the tracking component of the trigger, whereas the uncertainty due to the neutral component of the trigger is negligible. Therefore, the systematic error due to the trigger has been evaluated with a subsample of our data that satisfies the neutral as well as the tracking component of the trigger.

With these systematic errors added in quadrature and using the sign of  $h_{\nu\tau}$  determined in Refs. [7,8] we obtain the results listed in Table III. The results are in agreement with the standard  $V-A$  interaction.

## V. INTERPRETATION AND SUMMARY

The measurement of  $\xi$  and  $\delta$  implies that the probability  $P_R^\tau$  [see Eq. (3)] of a right-handed  $\tau$  to participate in leptonic  $\tau$  decays is  $P_R^\tau < 0.044$  at a 90% confidence level. Separately for electrons and muons, we obtain  $P_R^\tau < 0.066$  for the electronic mode and  $P_R^\tau < 0.067$  for the muonic mode. Both limits are at a 90% confidence level.

The 90% confidence limits on the reduced coupling constants  $g_{\epsilon\mu}^{\gamma'} = g_{\epsilon\mu}^{\gamma} / \max(g_{\epsilon\mu}^{\gamma})$  obtained from the combined results on the Michel parameters (Table III) are plotted in Fig. 4. Without directly measuring the helicity of the  $\tau$  neutrino in leptonic decays, the  $g_{LL}^S$  coupling cannot be distinguished from the  $g_{LL}^V$  coupling. Adding the knowledge of the param-



TABLE II. Contributions to the systematic error.

| Source   | $\Delta(\rho_e)$ | $\Delta(\rho_\mu)$ | $\Delta(h_{\nu_\tau}\xi_e)$ | $\Delta(h_{\nu_\tau}\xi_\mu)$ | $\Delta(h_{\nu_\tau}\xi_e\delta_e)$ | $\Delta(h_{\nu_\tau}\xi_\mu\delta_\mu)$ | $\Delta(h_{\nu_\tau}^2)$ |
|--|------------------|--------------------|-----------------------------|-------------------------------|-------------------------------------|---|--------------------------|
| Monte Carlo statistics                                   | $\pm 0.0025$     | $\pm 0.0028$       | $\pm 0.0122$                | $\pm 0.0131$                  | $\pm 0.0090$                        | $\pm 0.0072$                            | $\pm 0.0014$             |
| lepton identification                                    | $\pm 0.0006$     | $\pm 0.0033$       | $\pm 0.0005$                | $\pm 0.0016$                  | $\pm 0.0004$                        | $\pm 0.0025$                            |                          |
| acceptance function of spin analyzer considered          | $\pm 0.0010$     | $\pm 0.0015$       | $\pm 0.0038$                | $\pm 0.0093$                  | $\pm 0.0036$                        | $\pm 0.0064$                            | $\pm 0.0047$             |
| background disregarded                                   | $\pm 0.0009$     | $\pm 0.0012$       | $\pm 0.0018$                | $\pm 0.0067$                  | $\pm 0.0008$                        | $\pm 0.0023$                            | $\pm 0.0022$             |
| background   | $\pm 0.0004$     | $\pm 0.0009$       | $\pm 0.0029$                | $\pm 0.0059$                  | $\pm 0.0011$                        | $\pm 0.0017$                            | $\pm 0.0005$             |
| parameter $\beta$ of $\rho'$ contribution                | $\pm 0.0002$     | $\pm 0.0002$       | $\pm 0.0012$                | $\pm 0.0025$                  | $\pm 0.0002$                        | $\pm 0.0002$                            | $\pm 0.0010$             |
| Michel parameter $\eta$ $\Delta(\eta_\mu) = \pm 0.091^a$ |                  | $\pm 0.0170$       |                             | $\pm 0.0144$                  |                                     | $\pm 0.0125$                            |                          |
| Michel parameter $\eta$ $\Delta(\eta_\mu) = \pm 0.261^a$ | $\pm 0.0448$     |                    | $\pm 0.0417$                |                               | $\pm 0.0302$                        |   |                          |
| detector resolution                                      | $\pm 0.0004$     | $\pm 0.0004$       | $\pm 0.0006$                | $\pm 0.0005$                  | $\pm 0.0003$                        | $\pm 0.0004$                            | $\pm 0.0002$             |
| radiation  | $\pm 0.0013$     | $\pm 0.0011$       | $\pm 0.0018$                | $\pm 0.0032$                  | $\pm 0.0021$                        | $\pm 0.0041$                            | $\pm 0.0007$             |
| trigger  | $\pm 0.0017$     | $\pm 0.0035$       | $\pm 0.0094$                | $\pm 0.0123$                  | $\pm 0.0022$                        | $\pm 0.0025$                            | $\pm 0.0011$             |
| total $\Delta(\eta_\mu) = \pm 0.091^a$                   | $\pm 0.004$      | $\pm 0.018$        | $\pm 0.016$                 | $\pm 0.027$                   | $\pm 0.010$                         | $\pm 0.017$                             | $\pm 0.006$              |
| total $\Delta(\eta_\mu) = \pm 0.261^a$                   | $\pm 0.004$      | $\pm 0.045$        | $\pm 0.016$                 | $\pm 0.047$                   | $\pm 0.010$                         | $\pm 0.032$                             | $\pm 0.006$              |

<sup>a</sup>Reference [17].

eter  $\eta$  does not improve the limits. The couplings with a right-handed  $\tau$ ,  $g_{eR}^\gamma$ , are mostly constrained by the determination of  $\xi$  and  $\delta$ . Additional information comes from the measurement of  $\rho$ , which allows one to constrain the  $g_{RL}^V$  and  $g_{RL}^T$  couplings. Compared to the situation five years ago when only the Michel parameter  $\rho$  was measured in  $\tau$  decay and no limits on the coupling constants  $g_{e\mu}^\gamma$  existed, Fig. 4 illustrates the progress made. However, the  $V-A$  interaction as assumed by the standard model is still not fully experimentally verified for  $\tau$  decays.

More stringent limits can be obtained by restricting the generality of the model. For example, we consider a left-right symmetric model [28] for the electroweak interaction, where the parity violation has its origin in a spontaneous symmetry breaking of the left-right symmetry. In addition to

the pure left-handed  $W$  boson  $W_L$  of the standard model, such a model assumes a pure right-handed  $W$  boson  $W_R$ , where the mass eigenstates  $W_1$  and  $W_2$  are in general superpositions of the weak eigenstates  $W_L$  and  $W_R$ . This model can be parametrized by the mass ratio  $\alpha = M_1/M_2$  of the two bosons  $W_{1/2}$  and the mixing angle  $\zeta$  between  $W_{L/R}$ . The standard model is obtained in the limit  $\alpha \rightarrow 0$  and  $\zeta \rightarrow 0$ .

Figure 5 shows the one, two, and three  $\sigma$  contours for  $\alpha$  and  $\zeta$  obtained with the combined results on  $\rho$ ,  $\xi$ ,  $\xi\delta$ , and  $h_{\nu_\tau}$ . For  $\zeta=0$ ,  $W_2$  is identical with  $W_R$  and the following limit is obtained on  $M_R$ :

$$M_R > 304 \text{ GeV}/c^2 \text{ at } 90\% \text{ C.L.}$$

The mass limit obtained for  $\zeta$  free is

TABLE III. Results.  $\rho$ ,  $\xi$ , and  $\xi\delta$  denote the combined results.  $\rho_l$ ,  $\xi_l$ , and  $\xi_l\delta_l$  are the results separated for electrons and muons.

| Parameter           | World average [23] | This analysis <sup>a</sup>   | Correlation coefficients                 |  |
|---------------------|--------------------|------------------------------|--|--|
| $h_{\nu_\tau}$      | $-1.011 \pm 0.027$ | $-0.995 \pm 0.010 \pm 0.003$ |  |  |
| $\rho$              | $0.742 \pm 0.027$  | $0.747 \pm 0.010 \pm 0.006$  | $\kappa(\rho, \xi) = 0.046$              | $\kappa(\rho, \xi\delta) = 0.069$                  |
| $\xi$               | $1.03 \pm 0.12$    | $1.007 \pm 0.040 \pm 0.015$  | $\kappa(\rho, h_{\nu_\tau}) = 0.000$     | $\kappa(\xi, \xi\delta) = 0.158$                   |
| $\xi\delta$         | $0.76 \pm 0.11$    | $0.745 \pm 0.026 \pm 0.009$  | $\kappa(\xi, h_{\nu_\tau}) = -0.241$     | $\kappa(\xi\delta, h_{\nu_\tau}) = -0.276$         |
| $\rho_e$            | $0.736 \pm 0.028$  | $0.747 \pm 0.012 \pm 0.004$  | $\kappa(\rho_e, \xi_e) = 0.046$          | $\kappa(\rho_e, \xi_e\delta_e) = 0.074$            |
| $\xi_e$             | $1.03 \pm 0.25$    | $0.979 \pm 0.048 \pm 0.016$  | $\kappa(\rho_e, h_{\nu_\tau}) = 0.000$   | $\kappa(\xi_e, \xi_e\delta_e) = 0.216$             |
| $\xi_e\delta_e$     | $1.11 \pm 0.18$    | $0.720 \pm 0.032 \pm 0.010$  | $\kappa(\xi_e, h_{\nu_\tau}) = -0.194$   | $\kappa(\xi_e\delta_e, h_{\nu_\tau}) = -0.214$     |
| $\rho_\mu$          | $0.74 \pm 0.04$    | $0.750 \pm 0.017 \pm 0.045$  | $\kappa(\rho_\mu, \xi_\mu) = 0.026$      | $\kappa(\rho_\mu, \xi_\mu\delta_\mu) = 0.029$      |
| $\xi_\mu$           | $1.23 \pm 0.24$    | $1.054 \pm 0.069 \pm 0.047$  | $\kappa(\rho_\mu, h_{\nu_\tau}) = 0.000$ | $\kappa(\xi_\mu, \xi_\mu\delta_\mu) = -0.030$      |
| $\xi_\mu\delta_\mu$ | $0.71 \pm 0.15$    | $0.786 \pm 0.041 \pm 0.032$  | $\kappa(\xi_\mu, h_{\nu_\tau}) = -0.128$ | $\kappa(\xi_\mu\delta_\mu, h_{\nu_\tau}) = -0.152$ |

<sup>a</sup>Together with the sign of  $h_{\nu_\tau}$  determined in [7,8].

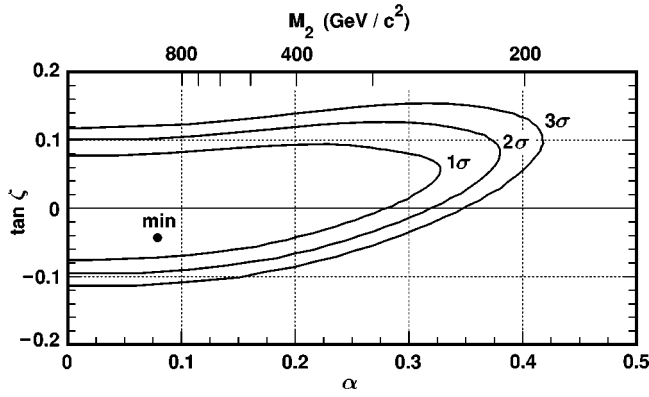


FIG. 5. Limits on the mass ratio  $\alpha$  and the mixing angle  $\zeta$  of a left-right symmetric model.

$$M_2 > 260 \text{ GeV}/c^2 \text{ at } 90\% \text{ C.L.}$$

The corresponding likelihood functions are shown in Fig. 6. The limit obtained in muon decay is  $M_2 > 406 \text{ GeV}/c^2$  [23].

We have also studied the constraints given by our measurement on extensions of the standard model with charged Higgs bosons. The  $\tau^-$  lepton and the charged daughter lepton  $l^-$  in leptonic  $\tau$  decays mediated by charged Higgs bosons are right handed [29,30]. Thus, in the general ansatz of Eq. (1), charged Higgs bosons are represented by the  $g_{RR}^S$  coupling. From our measurement on  $\xi_\mu$  and  $\xi_\mu \delta_\mu$  we obtain

$$M_{H^\pm} > 0.91 \times \tan\beta \text{ GeV}/c^2 \text{ at } 90\% \text{ C.L.},$$

where  $\beta$  is the ratio of vacuum expectation values. The combined limit obtained from this measurement and the recent CLEO measurement of  $\eta$  [17] is

$$M_{H^\pm} > 1.04 \times \tan\beta \text{ GeV}/c^2 \text{ at } 90\% \text{ C.L.}$$

All results presented here assume massless  $\tau$  neutrinos. We have studied the kinematical and dynamical effects of a 24-MeV/ $c^2$   $\tau$  neutrino on our results. We find that for the Michel parameters as well as for the  $\tau$  neutrino helicity the existence of such a neutrino would not affect the results at the level of our accuracy.

We have presented a precision measurement of the Michel parameters  $\rho$ ,  $\xi$ , and  $\delta$  in leptonic  $\tau$  decay as well as

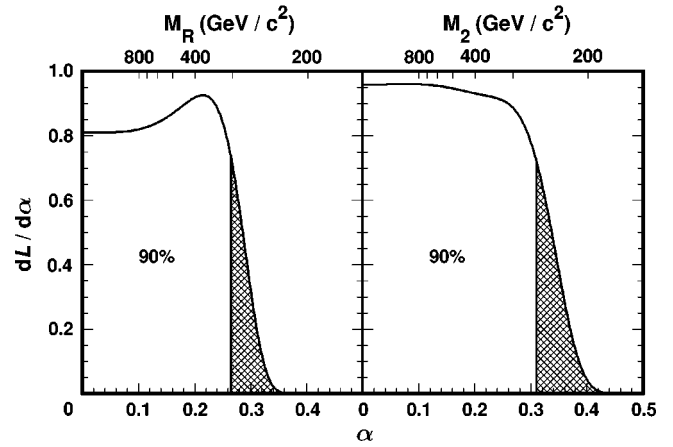


FIG. 6. 90% confidence limits on the mass ratio  $\alpha$  for (a)  $\tan\zeta=0$  and (b) for  $\tan\zeta$  free.

of the  $\tau$  neutrino helicity parameter  $h_{\nu_\tau}$ . The results obtained are consistent with the standard model prediction. With the exception of the Michel parameter  $\eta$ , the CLEO measurements given in Ref. [17] are superseded by the results obtained here. Despite the high statistics used, the accuracy of the measurements is still dominated by statistical and not systematic uncertainties. Thus there is potential to further improve the precision on the Michel parameters in  $\tau$  decays at the  $B$  factories soon to come into operation, as well as at future  $\tau$  factories.

#### ACKNOWLEDGMENTS

We gratefully acknowledge the effort of the CESR staff in providing us with excellent luminosity and running conditions. J.P.A., J.R.P., and I.P.J.S. thank the NYI program of the NSF; M.S. thanks the PFF program of the NSF; G.E. thanks the Heisenberg Foundation; K.K.G., M.S., H.N.N., T.S., and H.Y. thank the OJI program of the U.S. DOE; J.R.P., K.H., M.S., and V.S. thank the A.P. Sloan Foundation; A.W. and R.W. thank the Alexander von Humboldt Stiftung; and M.S. thanks Research Corporation for support. This work was supported by the National Science Foundation, the U.S. Department of Energy, and the Natural Sciences and Engineering Research Council of Canada.

[1] L. Michel, Proc. Phys. Soc. London, Sect. A **63**, 514 (1950).  
 [2] C. Bouchiat and L. Michel, Phys. Rev. **106**, 170 (1957).  
 [3] L. Okun and A. Rudik, Zh. Eksp. Teor. Fiz. **32**, 627 (1957) [Sov. Phys. JETP **6**, 520 (1957)].  
 [4] F. Scheck, Phys. Rep. **44**, 187 (1978); *Leptons, Hadrons, and Nuclei* (North-Holland, Amsterdam, 1983).  
 [5] S. Jadach, Z. Wąs, R. Decker, and J. H. Kühn, Comput. Phys. Commun. **76**, 361 (1993).  
 [6] Y. S. Tsai, Phys. Rev. D **4**, 2821 (1971).  
 [7] ARGUS Collaboration, H. Albrecht *et al.*, Z. Phys. C **58**, 61 (1993).  
 [8] ARGUS Collaboration, H. Albrecht *et al.*, Phys. Lett. B **349**, 576 (1995).

[9] ARGUS Collaboration, H. Albrecht *et al.*, Phys. Lett. B **246**, 278 (1990).  
 [10] ARGUS Collaboration, H. Albrecht *et al.*, Phys. Lett. B **316**, 608 (1993).  
 [11] SLD Collaboration, K. Abe *et al.*, Phys. Rev. Lett. **70**, 2515 (1993).  
 [12] ARGUS Collaboration, H. Albrecht *et al.*, Phys. Lett. B **337**, 383 (1994).  
 [13] ALEPH Collaboration, D. Buskulic *et al.*, Phys. Lett. B **321**, 168 (1994).  
 [14] ARGUS Collaboration, H. Albrecht *et al.*, Phys. Lett. B **341**, 441 (1995).

- [15] ALEPH Collaboration, D. Buskulic *et al.*, Phys. Lett. B **346**, 379 (1995).
- [16] L3 Collaboration, M. Acciari *et al.*, Phys. Lett. B **377**, 313 (1996).
- [17] CLEO Collaboration, R. Ammar *et al.*, Phys. Rev. Lett. **78**, 4686 (1997).
- [18] SLD Collaboration, K. Abe *et al.*, Phys. Rev. Lett. **78**, 4691 (1997).
- [19] S. Jadach and Z. Wąs, Acta Phys. Pol. B **15**, 1151 (1984).
- [20] M. Schmidler, Ph.D. thesis, Universität Karlsruhe, 1994.
- [21] S. Jadach and Z. Wąs, Comput. Phys. Commun. **36**, 191 (1985); **64**, 275 (1991); **85**, 453 (1995).
- [22] CLEO Collaboration, Y. Kubota *et al.*, Nucl. Instrum. Methods Phys. Res. A **320**, 66 (1992).
- [23] Particle Data Group, R. M. Barnett *et al.*, Phys. Rev. D **54**, 1 (1996).
- [24] M. Davier, L. Duflot, F. Le Diberder, and A. Rougé, Phys. Lett. B **306**, 411 (1993).
- [25] J. H. Kühn and A. Santamaria, Z. Phys. C **48**, 445 (1990).
- [26] L. M. Barkov *et al.*, Nucl. Phys. **B256**, 365 (1985).
- [27] J. Urheim, Nucl. Phys. B, Proc. Suppl. **55c**, 359 (1997).
- [28] M. A. B. Bég, R. V. Budny, R. Mohapatra, and A. Sirlin, Phys. Rev. Lett. **38**, 1252 (1977).
- [29] H. E. Haber, G. L. Kane, and T. Sterling, Nucl. Phys. **B161**, 493 (1979).
- [30] J. F. Gunion and H. E. Haber, Nucl. Phys. **B272**, 1 (1986).